Gain optimization of Er-doped fibers doped with Er:BaF_2 nanoparticles

Jennifer Campbell[1], Mary Ann Cahoon[2], Michael Gachich[1], Michael Norlander[1], Thomas Hawkins[2], John Ballato[2], Peter Dragic[1]

[1]University of Illinois Urbana-Champaign Holonyak Micro and Nanotechnology Laboratory, 208 N. Wright St., Urbana, IL 61801
[2]Clemson University Department of Materials Science and Engineering, 91 Technology Drive, Anderson, SC 29625
Author e-mail address: jjc11@illinois.edu, mcahoon@clemson.edu, mgachi2@illinois.edu, mgn3@illinois.edu, hawkin2@clemson.edu, jballat@clemson.edu, p-dragic@illinois.edu

Abstract: An Er:BaF_2 nanoparticle doped silica fiber (EDF) heavily doped with erbium exhibits mitigated quenching effects and possesses a high quantum efficiency (976 nm pumping). Investigations herein suggest the erbium concentration is scalable to 1 wt%.

1. Introduction

Erbium-doped fibers (EDFs) have been investigated for several decades for their excellent capabilities in optical amplification and lasing media [1]. EDFs are primarily valuable for systems operating in the telecommunications band centered at 1550 nm. Access to this wavelength range is possible due to the Er^{3+} emission from $^4I_{13/2} \rightarrow {}^4I_{15/2}$. However, erbium has two disadvantages as a dopant in silica. First, the absorption cross-sections are relatively low (compared, for example, to Yb^{3+}). Second, erbium solubility in silica is low and the ions are therefore prone to cluster. This clustering increases as the concentration of Er^{3+} increases [2]. As a result, when interested in high power fiber amplifiers, Yb-sensitization is often employed, where pumping into the $^4I_{13/2}$ band of Er^{3+} begins with the absorption of a photon by a Yb^{3+} and eventually transfers energy to an erbium ion [3].

Despite decades of research, Yb-free EDFs remain limited in their available doping concentration. As Er ions cluster, quenching of the ions (for example, either through ion-ion driven non-radiative decay or cooperative luminescence) negatively impacts the quantum efficiency (QE) of the fiber, resulting in a medium with less optical gain. While the quantum limit achievable for 1550 nm emission for a 976 nm pump is 63%, results reported in the literature have not yet reached within 10% of this value [4]. This paper presents preliminary deeply saturated gain measurements of the slope efficiencies for fibers doped with XEr:(100-X)BaF_2 nanoparticles for X=4,8. These results are compared to commercial highly doped, Yb-free fibers fabricated by Liekki and purchased from Thorlabs. The results presented herein show that the erbium concentration can be increased to over 1% by weight while maintaining QE above 50%. Results indicate that the presented QEs are scalable with optimization of the NP composition and its concentration in the fiber.

2. Fiber fabrication

The Er-doped BaF_2 nanoparticles (NPs) were synthesized in a liquid chemistry process similar to that reported in [5]. The first solution was the fluorinating solution and contained ammonium fluoride dissolved in diethylene glycol (DEG) at 90ºC under an N_2 atmosphere. The second solution contained barium acetate hydrate and erbium chloride hexahydrate at stoichiometric amounts to form Er-doped BaF_2 NPs with 4 and 8 mol% Er doping (NP 4 and NP 8, respectively). The Ba and Er precursors were dissolved in a DEG/water mixture. The Ba/Er solution was added to the fluorinating solution, reacted at 90ºC under N_2 atmosphere for 2h, and cooled to room temperature. This formed the "mother solution." The fiber was fabricated using mother solution diluted with equal parts DEG and doped to 0.05M Al_2O_3. In addition, the 8 mol% solution was made with a higher concentration of NPs (~twice that of NP 4).

The resultant suspension was doped into a fiber preform on an SG Controls MCVD lathe using a solution doping process equivalent to that employed for NP fibers reported in [6]. Cl was used during the drying steps to produce fibers with low OH levels. The preform was collapsed to ~15.5mm in diameter and drawn at ~1925ºC to ~125 μm diameter fiber with a custom Heathway draw tower. The fiber was coated with UV-curable high-index polymer (DSM 3471-3-14). Fiber composition was determined using energy-dispersive x-ray spectroscopy, refractive index using an IFA refractive index profiler, and attenuation using a PK2300 fiber analysis system.

3. Lifetimes and quantum efficiency

The measured slope efficiency of a laser is directly affected by the QE as $\eta_s = q_d\,\eta_q$, where q_d is the quantum limited slope efficiency ($q_d = \lambda_{pump}/\lambda_{signal}$, where λ is the wavelength of the pump or signal) and η_q is the QE. Measurements of the QE values quantify the impact of non-radiative effects such as quenching on the NP fibers. The QE was used as a comparator to two commercial EDFs of varying Er^{3+} concentration (Liekki Er30-4/125 [hereafter "Er 30"] and

Er110-4/125 ["Er 110"], with absorption values of 30 dB/m and 110 dB/m at 1530 nm, respectively). The peak absorption for the NP 4 and NP 8 fiber are 61 dB/m and 208 dB/m, respectively, also at 1530 nm.

The first method to estimate the QE was through measurements of the $^4I_{13/2} \rightarrow {}^4I_{15/2}$ upper state transition lifetime and applying appropriate integrations. The lifetime was measured by pumping approximately 2mm long fiber samples with a pulsed 976 nm diode laser. The emitted signal was filtered by one 1400 nm long-pass filter. The remaining fluorescence signal (near 1550 nm) was focused onto an InGaAs avalanche photodiode and measured as a function of time. Fig. 1 shows the normalized logarithmic (base-*e*) decay of the lifetime for each fiber. The curvature in each plot indicates that there is not a single type of Er^{3+} site that contributes to the upper state decay. The number of sites was determined using multi-term exponential fitting, in this case three. The first term is the slowest term, and the NP 4 and Er 30 fiber τ_{slow} values are assumed to be the radiative components of the lifetimes for the NP and commercial fiber families, respectively. The remaining two terms are faster and have significant non-radiative contributions due to quenching.

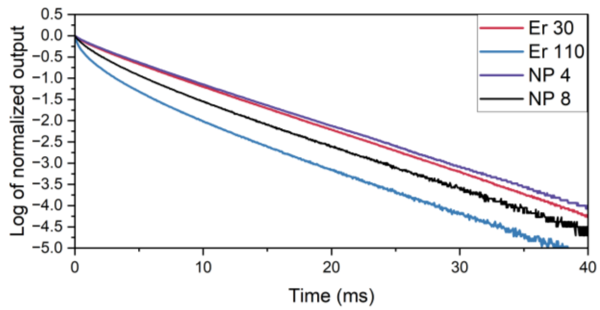

Fig. 1. 1550 nm lifetime plots for the NP fibers, the Er 30 commercial, and Er 110 commercial fibers. Decay is plotted as the logarithm of the normalized signal.

Table 1 shows the 1550 nm upper state lifetime data for all fibers. Each NP fiber had multiple samples taken and averaged to enumerate variance due to fluctuations in nanoparticle concentration along the length of the draw. Only one lifetime was taken for each of the commercial fibers, as variance from the doping method was not expected in the commercial process, and the available sample length was limited. These results reveal a similarity in τ_{slow} and QE between the lower concentration Er 30 commercial fiber and the NP 4 fiber despite the latter having about twice the erbium concentration. However, the Er 110 has a significantly lower QE, indicating sizeable quenching.

Table 1. Measured radiative and non-radiative lifetime values for each fiber. The last column is the calculated quantum efficiency from the lifetimes.

Fiber	τ_{slow}	τ_{nr1}	τ_{nr2}	η_q
Er 30	$10.28*10^{-3}$	$3.39*10^{-3}$	$4.55*10^{-4}$	0.84
Er 110	$8.72*10^{-3}$	$2.18*10^{-3}$	$2.91*10^{-4}$	0.43
NP 4	$10.68*10^{-3}$	$3.62*10^{-3}$	$5.18*10^{-4}$	0.80±0.03
NP 8	$9.71*10^{-3}$	$2.81*10^{-3}$	$4.71*10^{-4}$	0.54±0.003

4. Slope efficiency

1.1 Experimental setup

Measurements of the slope efficiency (SE) were performed with a three-stage erbium-doped fiber amplifier (EDFA) setup. A 1550 nm signal laser was combined with a 976 nm pump in the first and second stages, then amplified through commercial Er-doped fiber. In the final stage, the signal was combined with a third 976 nm pump with variable input power to measure the SE in the fiber under deeply saturated conditions. The output signal was then collimated through a lens, filtered of its residual pump, and directed into an integrating sphere detector and its power was measured as a function of increasing power of the third stage pump. Multiple tests were taken for each fiber to determine the optimal length, L_0, that maximized the SE value. The data presented herein is for the optimal length, measured via cutback on the sample.

There were three points of loss in the system that were measured to incorporate into the final calculation of SE for each fiber. First was the free space loss between the lens and detector. Second, the 976 nm pump leakage out of each sample at maximum operation of the amplifier (and therefore slope efficiencies are with respect to absorbed pump power). Third, the loss due to splicing the sample to the third stage. For the last measurement, splice loss was calculated by measuring the 976 nm output from the sample as a function of length (i.e., cutback) using only the maximum output of the third stage. Splice loss was largest in the Er 100 and NP 8 fibers. These losses were then incorporated into the SE measured from each test to calculate the adjusted SE.

1.2 Slope efficiency measurements and optimal fiber length

Fig. 2 plots the power curves for all fibers tested at their respective optimal lengths. The values for these optimal lengths and respective SE are listed in Table 2. The NP 4 fiber appears to have a comparable SE than the Er 30. Likewise, the NP 8 fiber appears to be similar in slope to the Er 110 fiber. The final calculation of SE is presented in Table 2. The NP 4 fiber resulted in an η_{slope} of 0.48. This exceeds the SE of Er 30. Similarly, NP 8 has an SE of 0.35, which is close to that of Er 110. With SEs comparable to commercial fibers but with twice the doping concentration, these NP fibers demonstrate a valuable first step towards developing short-length, low non-linearity EDFAs. There is an opportunity for the NP solution and Er concentration in the NP to be optimized to improve the SE and create a scalable method of developing these fibers.

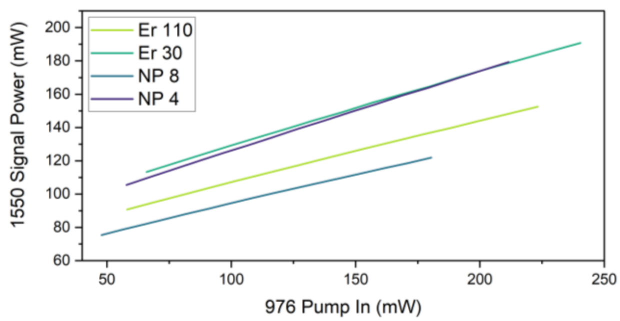

Fig. 2. Plot of output signal power versus absorbed pump power for each tested fiber at the optimal length.

Table 2. List of optimal lengths of operation for each EDF. For each length the adjusted slope efficiency after accounting for losses due to splicing, dispersion from the collimating lens, and pump leakage is presented. $\eta_{q,2}$ is the QE determined from η_{slope}.

Fiber	L_o (cm)	η_{slope}	$\eta_{q,2}$
Er 30	161.3	0.44	0.70
Er 110	38.15	0.37	0.59
NP 4	84.7	0.48	0.76
NP 8	19.6	0.35	0.56

5. Conclusions and future work

This work presented a novel Er:BaF_2 nanoparticle doped fiber identifying a scalable path towards developing shorter EDFAs based on highly erbium doped fibers with slope efficiencies that meet or exceed modern commercial EDFs with lower erbium concentrations. The fabrication technique allows for a higher concentration of Er^{3+} while maintaining high efficiency and low ion quenching. From these results, other variants of the nanoparticle solutions have been made to understand the scalability of the doping process. These variants increased both the concentration of Er in the nanoparticle and the amount of nanoparticles in the solution. Measurements of the lifetimes and slope efficiency as a function of Er concentration (increasing both NP concentration and Er content within each NP) in these new fibers will be presented at the conference.

5. References

[1] M. Norouzi, P. Badeka, P. Chahande, and B. Briley, "A survey on rare earth doped optical fiber amplifiers," in *IEEE International Conference on Electro-Information Technology , EIT 2013*, Rapid City, SD, USA: IEEE, May 2013, pp. 1–11. doi: 10.1109/EIT.2013.6632719.

[2] J. Nilsson, P. Blixt, B. Jaskorzynska, and J. Babonas, "Evaluation of parasitic upconversion mechanisms in Er/sup 3+/-doped silica-glass fibers by analysis of fluorescence at 980 nm," *J. Light. Technol.*, vol. 13, no. 3, pp. 341–349, Mar. 1995, doi: 10.1109/50.372427.

[3] Y. Hu *et al.*, "Performance of high-concentration Er/sup 3+/-Yb/sup 3+/-codoped phosphate fiber amplifiers," *IEEE Photonics Technol. Lett.*, vol. 13, no. 7, pp. 657–659, Jul. 2001, doi: 10.1109/68.930405.

[4] L.-C. Michaud *et al.*, "100-W-level single-mode ytterbium-free erbium fiber laser," *Opt. Lett.*, vol. 46, no. 10, p. 2553, May 2021, doi: 10.1364/OL.427291.

[5] M. A. Cahoon *et al.*, "(INVITED)On the evolution of nanoparticles in nanoparticle-doped optical fibers," *Opt. Mater. X*, p. 100202, Oct. 2022, doi: 10.1016/j.omx.2022.100202.

[6] P.-B. Vigneron *et al.*, "Anti-Stokes fluorescence cooling of nanoparticle-doped silica fibers," *Opt. Lett.*, vol. 47, no. 10, p. 2590, May 2022, doi: 10.1364/OL.457206.